Journal of Statistical Mechanics: Theory and Experiment
An IOP and SISSA journal

Visualization of avalanches in magnetic thin films: temporal processing

Alessandro Magni[1], **Gianfranco Durin**[1,2], **Stefano Zapperi**[2,3] **and James P Sethna**[4]

[1] Istituto Nazionale di Ricerca Metrologica (INRiM), Strada delle Cacce, 91-10135 Torino, Italy
[2] ISI foundation, Viale S Severo 65, 10133 Torino, Italy
[3] CNR-INFM National Center on nanoStructures and bioSystems at Surfaces (S3), Department of Physics, University of Modena and Reggio Emilia, Via Campi 213/A, 41100 Modena, Italy
[4] LASSP, Physics Department, Clark Hall, Cornell University, Ithaca, NY 14853-2501, USA
E-mail: magni@inrim.it, durin@inrim.it, stefano.zapperi@unimore.it and sethna@lassp.cornell.edu

Received 10 June 2008
Accepted 7 July 2008
Published 5 January 2009

Online at stacks.iop.org/JSTAT/2009/P01020
doi:10.1088/1742-5468/2009/01/P01020

Abstract. Magneto-optical methods allow us to observe the dynamics of domain wall motion, but this is intrinsically a very noisy process. We discuss a new method allowing us to reduce the measurement noise, taking advantage of the acquisition of a whole temporal sequence of images.

The resulting avalanche distributions give interesting hints as to the magnetization dynamics, but are strongly dependent on the size of the observation windows chosen. We investigate the effects of window size by studying finite-size scaling, and use this to extract the fractal dimension critical exponent $1/\sigma\nu$.

Keywords: critical exponents and amplitudes (experiment), interfaces in random media (experiment)

Contents

1. Introduction

For every magnetic substance, the material volume is subdivided into regions where the magnetization points homogeneously in the same direction: these *magnetic domains* are separated by *domain walls*. In the large majority of magnetic materials these walls exhibit a motion characterized by abrupt transitions. The resulting noise—Barkhausen noise—is a basic example of complexity in materials science, and has been the subject of a long and continuing series of studies.

There are two possible ways of investigating this motion: using fluxometric measurements and using magneto-optical measurements. In the fluxometric setup the motion of the domain walls is measured as an induced voltage in a secondary coil: this voltage is a measure of the cumulative effect of the magnetization variation throughout the sample volume. In the magneto-optical methods, instead, the magnetic domains themselves are observable, so an acquisition sequence leads to the visualization of the motion of the domain walls present in the observation field. It can be clearly recognized how much more information can be gathered via magneto-optics, due to the possibility of directly observing the spatial motion of the interfaces in time. Yet, we will see in the article that the information gathered by this method, if it is not carefully processed, can lead to important misunderstandings.

The domain wall motion in bulk systems has been studied for a long time. In such systems the domain wall structure is the classical *Bloch wall* structure, where the magnetization rotates to avoid creating magnetic charges on the wall surface. Most of the statistical properties of this motion are now understood in terms of a depinning transition of the domain wall, and many experimental results are well explained by these theories [1]. In thin films, the motion of walls is presumably dominated by depinning as well, but our understanding of the dynamics is still at a preliminary stage. A possible source of complexity in two-dimensional systems is the domain walls changing their structure as a function of the system thickness. Very generally, we can say that as the thickness decreases, the wall passes through the stages of *Bloch wall*, *asymmetric Néel wall*, *cross-tie wall*, and *Néel wall* [9]. These interfaces have different internal magnetic structures, so we can expect the statistical properties of their motion to be different too. Moreover, their structure is more complex than simple Bloch walls, and the dominant interactions

J. Stat. Mech. (2009) P01020

important for the wall dynamics are much more complicated. Also, from the experimental point of view, the data available are still limited, although the few recent papers published using the magneto-optical Kerr effect have shown interesting and promising results. In 2000, Puppin [2] measured the critical exponent τ of the avalanche size distribution $P(S) \sim S^{-\tau} f(S/S_0)$ in a Fe/MgO film of 90 nm to be about $\tau \sim 1.1$, much less than the values reported in the literature for bulk systems. Later, Kim *et al* [3] did indeed measure larger values $\tau \sim 1.3$ in Co thin films of different thicknesses (5–50 nm). Very recently, Ryu *et al* [4] have argued that in a 50 nm MnAs film on GaAs(001), having a Curie temperature of only about 45 °C, there is a crossover between different universality classes driven by temperature, with the exponent τ continuously changing from 1.32 to 1.04 as the temperature is increased from 20 to 35 °C. All of these experiments rely upon measuring avalanches magneto-optically, in a small region of the entire sample. Usually, different enlargements are used, and the distributions are superimposed to fit the critical exponent τ over a few decades. In all these experiments, the effect of the window size on the avalanche statistics has not been incorporated into the analysis—e.g., the dependence of the distribution cutoff S_0 on the window size.

In this paper, we aim to explore some experimental issues associated with extracting avalanche statistics from optical data. (Some of the material here has been presented before [5].) First, we need to set up reliable methods for extracting avalanche distributions from a series of optical images, properly taking into account the effect of background noise. This is clearly the central issue for being able to determine accurate critical exponents. Secondly, we need to investigate the proper scaling approach to address the finite-size cutoff in the avalanche sizes induced by the observation window. In particular, we will use the effects of the window size on simulated data to illustrate how to estimate the critical exponent $1/\sigma\nu$ governing the fractal dimension of the avalanches.

2. Avalanche distributions from a sequence of Kerr images

The determination of avalanche sizes using magneto-optics is not simple as compared with making fluxometric measurements, which are especially suitable for bulk materials [1]. In fluxometric measurements, in fact, one detects the change of magnetization in time via the induced voltage in a secondary coil: this voltage is a measure of the cumulative effect of the magnetization variation throughout the sample volume. Avalanches have a different weight, however: avalanches originating farther from the coil generate a lower signal, with a decay length $x_0 \propto \sqrt{\mu}$, where μ is the permeability [10]. But the advantage is that each avalanche is measured in full—although its weight is reduced if it happens far from the coil. In the output signal V(time), to separate distinct avalanches one simply introduces a voltage noise threshold, which experimentally sets the beginning and end of the avalanche.

In this work we will make use of a magneto-optical effect—the longitudinal Kerr effect. The magneto-optical effect consists of a small rotation of the polarization plane of the light incident on a magnetized sample. The direction of this rotation is related to the local magnetization. Using a polarization microscope one is thus able to obtain a grayscale image where the local gray value is directly related to the magnetization—in the case of the longitudinal Kerr effect, to the in-plane component, in the direction of the applied field. With increasing applied field one usually observes the motion of an interface (the domain wall) sweeping in one direction, as ever larger portions of the sample invert

J. Stat. Mech. (2009) P01020

their local magnetization. Since the maximum rotation angle is very low (usual values are below 0.5°) this kind of measurement is very noisy. Clearly, it is challenging to separate signal from noise in the richer space–time information provided by the sequence of Kerr images. The challenge is to find the space–time surface $\Gamma(x, y)$ separating the inverted from the non-inverted regions. This problem is particularly important when extracting avalanche size distributions, where the small avalanches are crucial for estimates of the critical exponents.

To address this question, we acquired images of the motion of zigzag domain walls [9] on Permalloy thin films (with 170 nm thickness), using the high-resolution longitudinal Kerr effect, with the sample magnetized by a slowly varying longitudinal in-plane field. The microscope is a Zeiss Axioscop2 Plus, modified with additional optical elements to obtain a parallel s-polarized light beam exiting the objective, and with an off-axis aperture stop in the objective back-focal plane to obtain the correct Kerr angle of the light beam. The magnification is given by 20× and 10× objectives (with numerical aperture 0.40 and 0.25 respectively) which allow us to acquire images having sizes 480 μm × 340 μm and 880 μm × 660 μm. The microscope uses a Zeiss Axiocam HRm camera (14 bit, Peltier cooled), whose main bottleneck arises from the time needed (about 0.5–0.8 s) to transfer successive frames to the computer for storage. The field is applied with Helmholtz coils, which allow the application of fields up to ≈20 kA m^{-1} along the light incidence plane. The observations are made under a sinusoidally varying field, with $f = 1$ mHz.

As usual with images obtained by in-plane Kerr effect, the contrast of the unprocessed images is fairly low. Therefore, prior to acquisition, a reference state is captured at saturation. After the run, the reference state is subtracted from each image to allow the observation of the magnetic state variation only. Following this procedure, we now need to clearly identify the domains in the images.

Among the standard techniques [6, 7], smoothing is used to deal with low amounts of noise: it is equivalent to the suppression of high frequencies in the frequency domain. Unfortunately, it also blurs the sharp edges of the domain walls, that are the most important feature that we are looking for. Another possibility is to apply to the image $I(i, j)$ a convolution with a kernel $K(m, n)$, obtaining a filtered image $O(i, j) = \sum_{k,l} K(k, l)I(i - k, j - l)$: this is a general technique that—depending on the kernel used—can lead to different types of filters, from sharpening to edge detection, to Gaussian smoothing and so on. Another processing method consists in making use of morphological operators (open/close, erode/dilate, tophat). In this case a grayscale extremum operation is performed over a small neighborhood defined by the structuring element (analogous to the kernel in the convolution): these operations are in general able to reduce the noise by using the spatial information around each pixel.

As a matter of fact, all the procedures described can be problematic, a major stumbling block being the remaining non-homogeneity of the illumination in the field of view. Moreover, these methods fail especially in identifying the small avalanches. The general point is that by analyzing each image in isolation, we lose the useful information provided by the time sequence.

Instead, a simple but effective starting point is to ignore the spatial information and consider only the evolution in time for each pixel. The camera acquires in grayscale, and a given pixel value will have noisy fluctuations around a value I_- at early times, switching to fluctuations around I_+ when the magnetization front passes past the

J. Stat. Mech. (2009) P01020

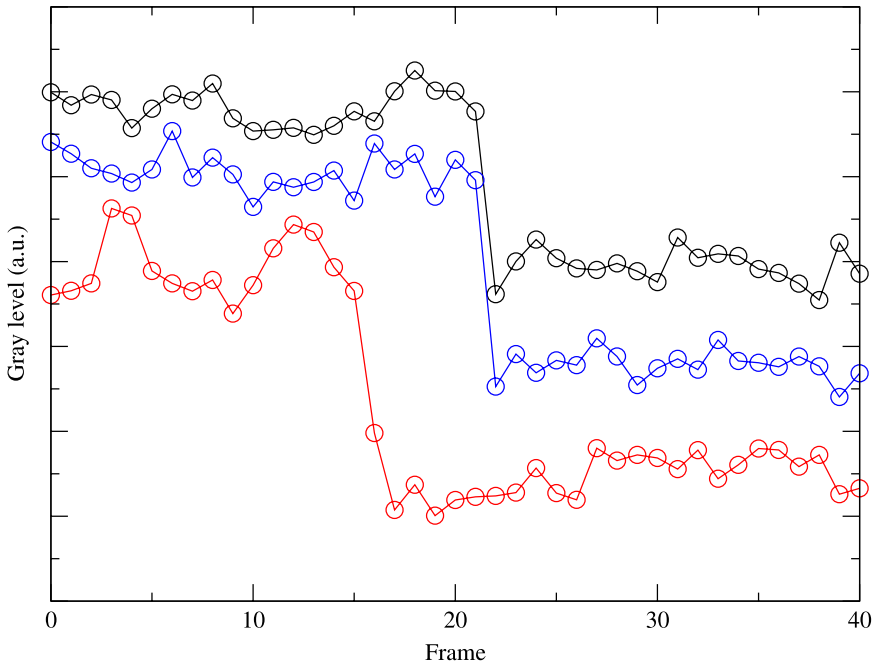

Figure 1. Time sequences of the grayscale for three adjacent pixels in a magneto-optical image. Visual inspection clearly reveals the black and blue pixels as having the same switching time, but numerical calculation can give spurious results due to the noise of the sequences and the reduced change of the gray level.

pixel at a time t_0. Here I_- and I_+ depend upon local inhomogeneities in color and upon the average illumination in that region. The noise level is so high that the fluctuations can occasionally cross the mid-point $(I_-+I_+)/2$ prior to the effective switching time t_0.

In figure 1, we report an example of the gray intensity of three adjacent pixels, where two of them switch at the same time, while the third (red) switches at an earlier time. Detecting the correct switching time t_0 by taking the numerical derivative of the signal gives spurious answers. We adopted instead a series of routines with different levels of smoothing of the signal and successive derivative calculation.

The result of this calculation is the switching time matrix $\Gamma(x, y)$ whose values represent the switching time at each point. We are then able to reconstruct the filtered images through time, defining—in the image at time t_0—the pixel (x, y) as being negatively saturated if $t_0 < \Gamma(x, y)$, positively saturated otherwise.

Inevitably we found that a small but non-negligible number of pixels still appear to switch at the wrong time. To correct for this, we also took advantage of the spatial information, using algorithms that adjust the switching time to that of adjacent pixels if they appear to be in the same avalanche except for small noise. These methods are pretty delicate, as they can reduce or eventually destroy small avalanches, which, as said, are essential for critical exponent estimation.

An example of avalanche visualization is shown in figure 2, where we use the same color palette (from red to blue) as was used by [4] for ease of comparison. On the left, we show the jump sequence for a field of view of 880 μm $\times$ 660 μm, in which we did

J. Stat. Mech. (2009) P01020

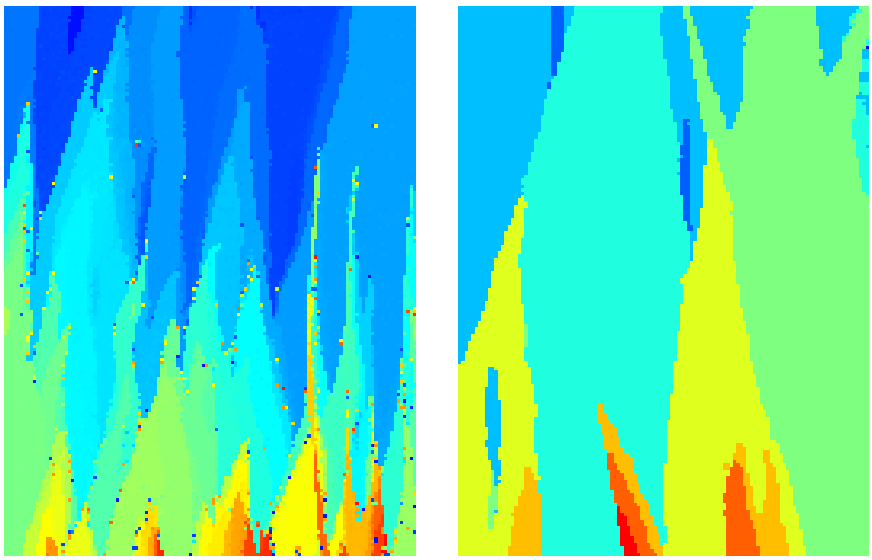

Figure 2. Jump sequences on a 170 nm permalloy thin film at two fields of view (880 μm $\times$ 660 μm (left), and 440 $\times$ 330). The magnetic field direction is vertical. The color code represents the time at which the jump occurs (from red to blue).

not apply any spatial correction to the pixels, so a certain number of incorrect switches are shown. In any case, the sequence of zigzag domains is well detected, showing the jerky character of domain wall motion. On the right, taken at a larger magnification (480 μm $\times$ 340 μm), we do apply the spatial correction, giving a significant decrease of incorrect switches.

3. Multiscale measurements of avalanche distributions: varying the window size

In the comparison of the two images in figure 2, it is clear not only that different fields of view detect different details of the domain wall jumps, but, notably, that large jumps that overlap window boundaries are chopped, and so may be counted as smaller avalanches in smaller frames. In particular, the size of the window has a strong influence on the largest avalanche size which can be detected. Given that the best experiments can only measure two or three decades of avalanche sizes for a given window, it would be valuable to combine information from several window sizes. This avalanche chopping effect is absent in the fluxometric methods, that integrate the complete signal of each avalanche. In the magneto-optical setup instead we must check to be sure that the inclusion in the statistics of partial avalanches does not create errors in the critical indices. We must therefore understand the finite-size effects with windowed boundary conditions.

To explore the effect of window size on the avalanche distributions, we consider a model for a domain wall moving in a random environment. We chose a simple enough model, allowing just the freedom to change the interface roughness as a function of one parameter—we do not intend yet to model the zigzag domain walls in thin films. While the model is not completely realistic in terms of the experiments, it provides a prototypical description of a self-affine interface moving in a disordered landscape. The equation of

J. Stat. Mech. (2009) P01020

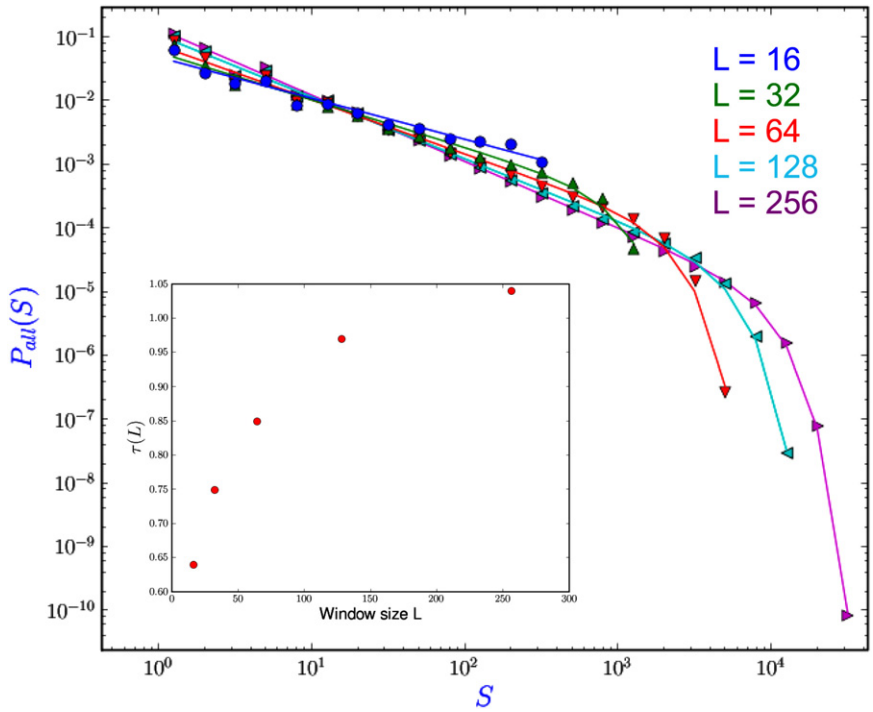

Figure 3. Distribution of avalanche sizes inside windows of different sizes L, including all avalanches (including the chopped portions of avalanches which cross the borders of the windows). The inset shows the change of the fitted exponent τ with the window size L, approaching the theoretical value of $\tau = 1.18$ only for large sizes.

motion for the domain wall is given by

$$\frac{\mathrm{d}h(x,t)}{\mathrm{d}t} = H - k\bar{h} + \nu\frac{\mathrm{d}^2h}{\mathrm{d}x^2} + \lambda\frac{\mathrm{d}}{\mathrm{d}x}\left(\frac{\mathrm{d}h}{\mathrm{d}x}\right)^3 + \eta(x,h), \tag{1}$$

where $h(x,t)$ is the position of the domain wall, $\bar{h}$ is the center of mass of the wall that is proportional to the magnetization, $H(t)$ is a slow varying external field, k is the demagnetizing factor, $\nu\mathrm{d}^2h/\mathrm{d}x^2$ is the domain wall linear stiffness to which we added a small non-linear correction controlled by λ, and $\eta(x,h)$ is a random field describing all the inhomogeneities present in the sample. The effect of the non-linearity is crucial in two dimensions since otherwise the model would display anomalous scaling with super-rough behavior [8]. We simulate a cellular automaton version of equation (1) where time and space are discretized and the local velocity can assume only the values 0 or 1. The model displays an avalanche distribution with scaling exponent $\tau = 1.18 \pm 0.01$. The domain wall is found to be self-affine with a roughness exponent $\zeta = 0.65 \pm 0.05$, in good agreement with the result $\zeta = 0.63$, reported in [8].

In order to compare the model with the experiments, we restrict our analysis to the avalanches (or avalanche fractions) occurring inside square windows of linear size $L = 16, 32, 64, 128, 256$, for a system of total width $L_{\mathrm{tot}} = 2048$.

A difficulty in the analysis of the data is that large avalanches near depinning transitions are increasingly anisotropic: an avalanche with width W will have typical

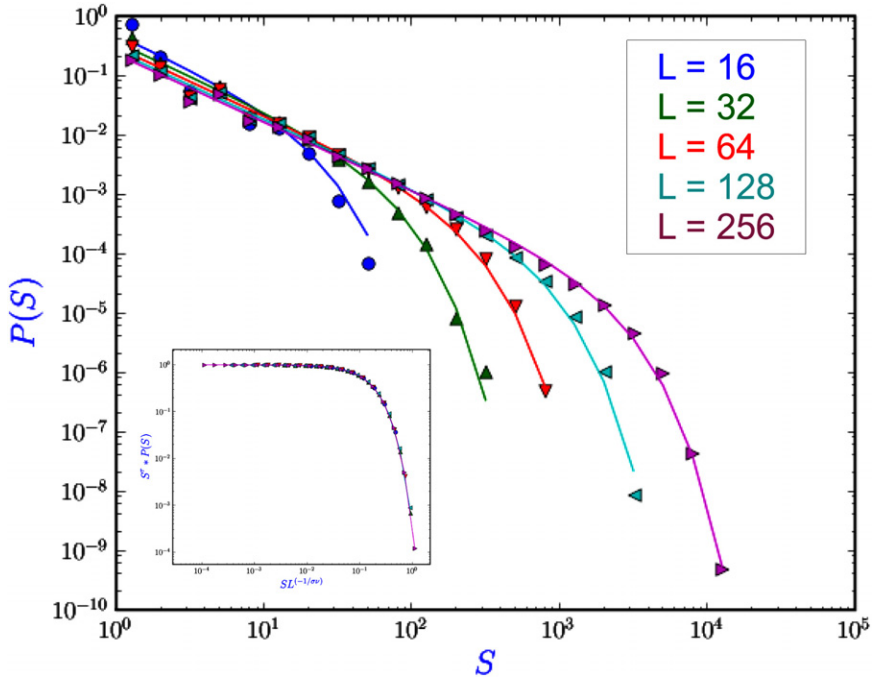

Figure 4. Distribution of avalanche sizes inside windows of different sizes L but not touching the borders of the windows. The inset shows the finite-size scaling collapse of $S^{\tau}P(S)$ as a function of $SL^{-1/\sigma\nu}$ (equation (2)) with $\tau = 1.19 \pm 0.10$, $1/\sigma\nu = 1.7 \pm 0.06$.

height $H \sim W^{\zeta}$. If $\zeta < 1$, as in the case of equation (1), large avalanches become short and fat. This means that the main effect of large windows is to cut off the widest avalanches, while at small window sizes a substantial number of tall avalanches may also be removed. Thus, unlike for isotropic finite-size scaling, the effects of larger windows are not similar to those of small windows: they are similar to those of smaller windows *of a different shape*.

We can analyze the data using the finite-size scaling form

$$P(S, L) = S^{-\tau}\mathcal{P}_W(S/L^{1/\sigma\nu}) \tag{2}$$

appropriate for systems with a strip geometry of width L and infinite height.

A first possible approach if to simply superimpose data coming from different window sizes (e.g. [2]). In this case we include also the chopped avalanches, originating from avalanches touching the window borders. The resulting distribution has an exponent τ monotonically increasing with window size, slowly approaching the theoretical value only at the largest window sizes (figure 3). The contribution of avalanches artificially chopped when crossing the side boundaries likely is introducing an important subdominant correction to the finite-size scaling. This effect, if also present in experiments at similar levels, could seriously interfere with extraction of good exponents from non-imaging magneto-optical methods that cannot discriminate against avalanches which touch the side boundaries [2].

A possible alternative is to incorporate in the calculations only avalanches that touch none of the borders of the window—avoiding the extra truncated avalanches. Possible

J. Stat. Mech. (2009) P01020

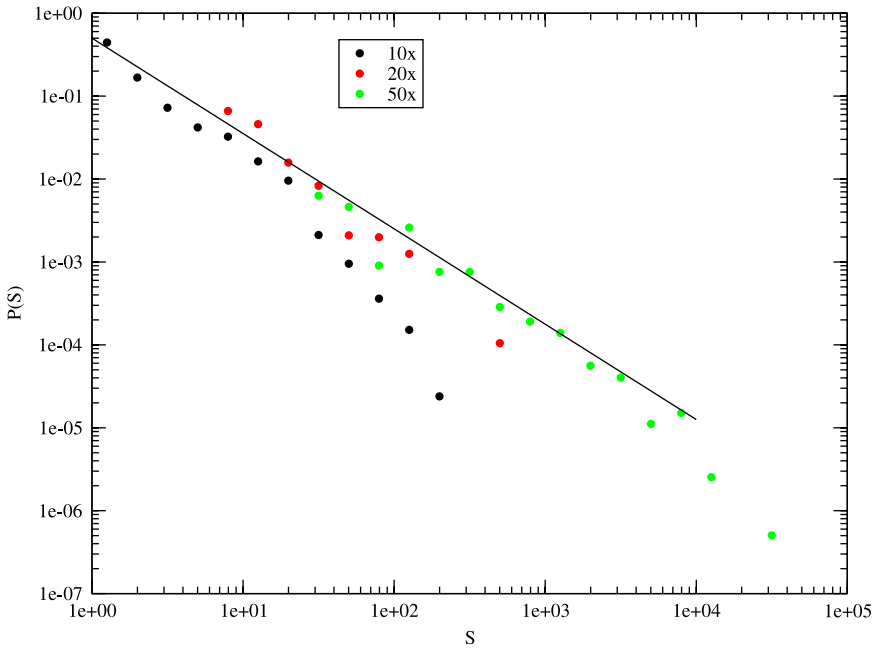

Figure 5. Distribution of measured avalanche sizes (preliminary data) for different magnifications 10×, 20×, 50×, using only those avalanches completely contained inside the window. The data set is compatible with an exponent $\tau = 1.15$.

problems can sometimes originate from the presence of residual noise, which can produce mistakes in the selection of avalanches not in contact with the borders.

Figure 4 shows the results of our simulations using this method, where only the avalanches that do not touch the sides of the $L \times L$ window are incorporated. Doing this, we find that the fitted exponents $\tau = 1.19 \pm 0.10$, $1/\sigma\nu = 1 + \zeta = 1.72 \pm 0.06$ are close to the theoretically expected values ($\tau \sim 1.18$ and $1/\sigma\nu = 1.63$). The data collapse of $S^{\tau}P(S)$ as a function of $SL^{-1/\sigma\nu}$ shows that the τ value remains constant at different L values; by avoiding avalanches which touch the boundaries, corrections to finite-size scaling are much reduced.

The analysis of experimental data is at a very preliminary stage, still optimizing the algorithm needed to correctly count only the avalanches inside the window, and to minimize loss of avalanches due to noise. In figure 5 we show an initial result, where a well defined common slope of the distributions is apparent, with the exponent $\tau \sim 1.15$.

4. Conclusions

The experimental and theoretical analysis shown here leads us to conclude that visualization measurements must be analyzed with care, since the estimated exponents can reflect the finite size of the windows. Indeed, by using a set of different magnifications one can use this windowing to advantage; finite-size scaling, for example, can be used to estimate a new critical exponents $1/\sigma\nu$.

doi:10.1088/1742-5468/2009/01/P01020

J. Stat. Mech. (2009) P01020

Acknowledgment

JPS would like to acknowledge NSF DMR-070167 for support.

References

[1] Durin G and Zapperi S, 2005 *The Science of Hysteresis: Physical Modeling, Micromagnetics, and Magnetization Dynamics* vol 2 (Amsterdam: Academic) chapter 3 (The Barkhausen Noise) p 181 [cond-mat/0404512]
[2] Puppin E, *Statistical properties of Barkhausen noise in thin Fe films*, 2000 *Phys. Rev. Lett.* **84** 5415
[3] Kim D-H, Choe S-B and Shin S-C, *Direct observation of Barkhausen avalanche in Co thin films*, 2003 *Phys. Rev. Lett.* **90** 087203
[4] Ryu K-S, Akinaga H and Shin S-C, *Tunable scaling behavior observed in Barkhausen criticality of a ferromagnetic film*, 2007 *Nat. Phys.* **3** 547
[5] Durin G, Magni A, Zapperi S and Sethna J P, *Avalanches through windows: multiscale visualization in magnetic thin films*, 2008 *IEEE Trans. Magn. Mater.* at press
[6] Schmidt F, Rave W and Hubert A, *Enhancement of magneto-optical domain observation by digital image processing*, 1985 *IEEE Trans. Magn.* **21** 1596
[7] Nixon M and Aguado A, 2002 *Feature Extraction and Image Processing* (Amsterdam: Elsevier)
[8] Rosso A and Krauth W, *Origin of the roughness exponent in elastic strings at the depinning threshold*, 2001 *Phys. Rev. Lett.* **87** 187002
[9] Hubert A and Schafer R, 2000 *Magnetic Domains* (Berlin: Springer)
[10] Alessandro B, Beatrice C, Bertotti G and Montorsi A, *Phenomenology and interpretation of the Barkhausen effect in ferromagnetic materials*, 1988 *J. Appl. Phys.* **64** 5355